Oxygen over stoichiometry in the 2 H-perovskite related structure: The route to a large family of cation deficient Ising chain oxides Sr 1+y [(Mn 1-x Co x) 1-z z]O 3

Vincent Caignaert, Olivier Perez, Philippe Boullay, Motin Seikh, Nahed Sakly, Vincent Hardy, Bernard Raveau

Oxygen over stoichiometry in the 2 *H*-perovskite related structure: The route to a large family of cation deficient Ising chain oxides $Sr_{1+y}[(Mn_{1-x}Co_x)_{1-z}\square_z]O_3$

Vincent Caignaert[1]*, Olivier Perez[1], Philippe Boullay[1], Md Motin Seikh[1,2], Nahed Sakly[1], Vincent Hardy[1] and Bernard Raveau[1]*

1- *Laboratoire CRISMAT, UMR 6508 CNRS-ENSICAEN, University of Caen, Bd du Maréchal Juin 14050 Caen cedex, France.*
2- Department of Chemistry, Visva-Bharati *University, Santiniketan–731235, West Bengal, India*

Corresponding authors:vincent.caignaert@ensicaen.fr, bernard.raveau@ensicaen.fr

Abstract: The realization of oxygen over stoichiometry through oxidation of Co^{2+} into Co^{3+} in the 2*H*-perovskite related oxides $Sr_{1+x}(Mn_{1-x}Co_x)O_3$ is demonstrated, leading to a large family of cation deficient Ising chain oxides $Sr_{1+y}[(Mn_{1-x}Co_x)_{1-z}\square_z]O_3$. In these aperiodic hexagonal structures also formulated $Sr_{1+x}(Mn_{1-x}Co_x)O_{3+\delta}$ ($a\approx9.6$ Å, $c_1\approx2.6$ Å, $c_2\approx3.9$ Å), and built up of face sharing octahedral and trigonal prismatic polyhedra, the observed modulation vector $\gamma=c_1/c_2$, (ranging from ~0.641 to ~0.668) allows the proportion of octahedral (N_O) and prismatic sites (N_P) to be obtained according to the relations: $y=2\gamma-1= N_P/(N_P+N_O)$. For these oxides, the rate of cationic vacancies (z) in the chains and the oxygen over-stoichiometry (δ) can be deduced from the relations: $z=(x-y)/(1+x)$ and $\delta=3(x-y)/(1+y)$. The analysis of these results shows that the structure of the chains, i.e. the proportion of tetrameric units "M_4O_{12}" coexisting with trimeric units "M_3O_9" is highly sensitive to the oxygen over-stoichiometry for a fixed cationic composition. This is illustrated here by the structure of the oxide corresponding to x=0.375 with $\delta=0.09$, which is commensurate with $\gamma=2/3$ similar to $Sr_4Mn_2CoO_9$ but with a significant content of cationic vacancies in the trigonal prismatic sites according to the formula $Sr_4(Mn^{IV}_{1.818}Co^{III}_{0.544}Co^{II}_{0.548}\square_{0.09})O_9$. Thus, the presence in those chains of cationic vacancies due to oxygen overstoichiometry appears as a very important concept which opens the route to the synthesis of fragmented chain structures and may have a huge impact upon the magnetic and magneto-electric behavior of Ising chain oxides.

Introduction

One dimensional alkaline earth manganates and cobaltates form a large family previously formulated as $A_{3m+3n}Co_nB_{3m+n}O_{9m+6n}$ (A=Ca, Sr, Ba, B= Mn, Co), whose chains consist of face-sharing CoO_6 trigonal prisms and CoO_6/MnO_6 octahedra [1-5]. Though these oxides offer a vast field for the investigation of magnetism, only few of them have been investigated except for the two first "m=0, n=1" members. Indeed $Ca_3Co_2O_6$, after the evidence for its particular magnetization steps behavior [6-12], has been later on investigated by many authors for the complex nature of its magnetism [13-24]. The other m=0, n=1 member, Ca_3CoMnO_6 was more recently studied for its particular magnetic order and its multiferroicity [25-29]. Besides, the "m=1,

n=3 members, $Sr_{4-x}Ca_xMn_2CoO_9$ whose structure was first discovered for $Sr_4Mn_2CoO_9$ [30] were recently shown to exhibit (for x=0-2) a great potential for the realization of new nanomagnets, i.e. single chain magnets (SCM) and single ion magnets (SIM) never observed before in condensed matter materials [31-33]. These features that are similar to those previously investigated in molecular compounds [34-37] open the route to potential applications in information storage and computation [38-40].

Thus, the recent evidence for SCM and SIM properties for the oxide $Sr_4Mn_2CoO_9$ whose commensurate chain structure consists of trimeric "Mn_2CoO_9"(Oh_2Tp) units of two MnO_6 octahedra Oh sharing faces with one CoO_6 trigonal prism Tp (**Fig.1a**) makes that the Sr-Mn-Co-O

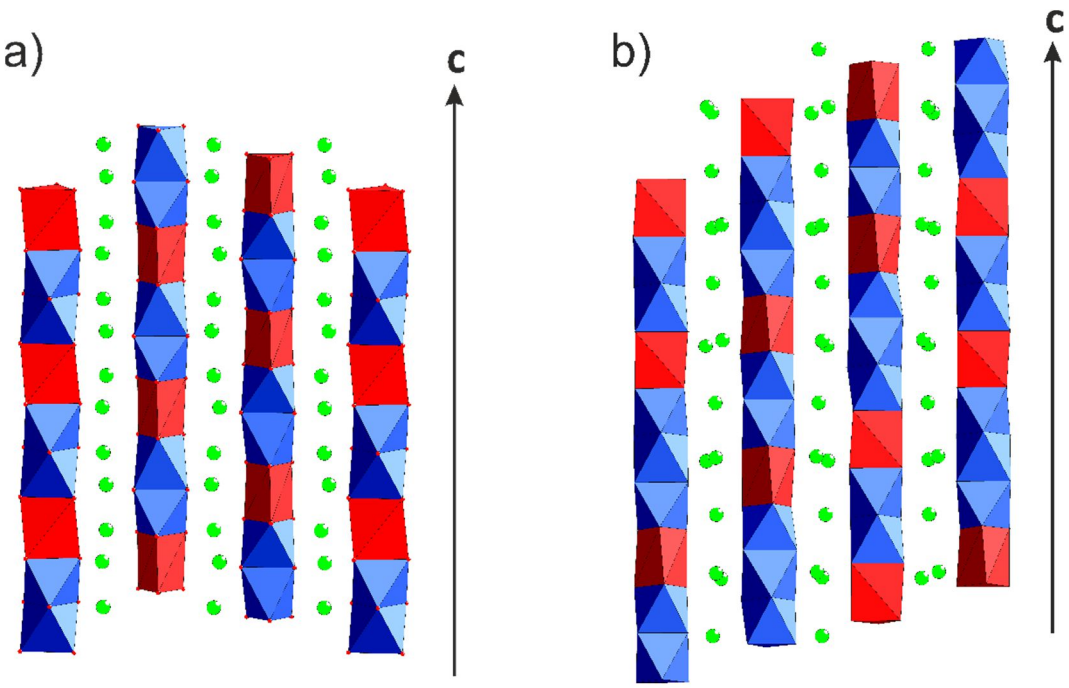

Fig.1 Structure of the commensurate oxides (a) $Sr_4Mn_2CoO_9$ and (b) $Sr_9Mn_5Co_2O_{21}$, stoichiometric members of the series $Sr_{1+x}(Mn_{1-x}Cox)O_3$ with x= 1/3 and x= 2/7 respectively. The trimeric and tetrameric units Oh_2Tp and Oh_3Tp consist of one trigonal CoO_6 (red colored) sharing faces with two or three MnO_6 octahedra (blue colored) respectively MnO_6 octahedra. Sr^{2+} cations are represented by green spheres.

system offers an attractive field for the investigation of other oxides with a closely related chain structure. Considering the key-structural model reported by Perez-Mato *et al* [2], the oxides $Sr_4Mn_2CoO_9$ (**Fig.1a**) and $Sr_9Mn_5Co_2O_{21}$ (**Fig.1b**) synthesized by Boulahya *et al* [30, 41] can indeed be described as the commensurate x=1/3 and x=2/7 members of a structural family $Sr_{1+x}(Mn_{1-x}Co_x)O_3$ whose crystal structure can be either commensurate or incommensurate

depending on the x value. In this way, Battle et al [42] demonstrated, using powder neutron diffraction, the existence of incommensurate modulated structures for x=0.266 and 0.280 (synthesized from nominal composition x=3/11(=0.2727) and x=2/7(=0.2857) respectively). This was shown to be due to the aperiodic distribution in the chains of trimeric "Mn_2CoO_9" ($M_2M'O_9$ or Oh_2Tp) units with tetrameric "Mn_3CoO_{12}" ($M_3M'O_{12}$ or Oh_3Tp) units built up of three MnO_6 octahedra sharing faces with one CoO_6 trigonal prism. Besides the oxides $Sr_{1+x}(Mn_{1-x}Co_x)O_3$ characterized by the "Mn^{4+}/Co^{2+}" valence, other incommensurate composite structures with a different generic formulation involving the valence "Mn^{4+}/Co^{3+}"were also obtained for Co-rich compositions [43-44].

In fact, the complex crystal chemistry of these oxides requires the oxygen non stoichiometry to be considered as a primordial parameter for their generation. Due to the synthesis in air, the possibility of oxygen over stoichiometry with respect to the nominal composition of the 2 *H*-perovskite related structure has been recently considered for explaining the effect of thermal treatment on the commensurability/incommensurability and magnetism of the parent spin chain oxide $Sr_3CaMn_2CoO_{9+\delta}$ [45], based on the behavior of the incommensurate oxides $Sr_3RhMO_{6+\delta}$, with M=Cu, Ni, Zn [46-47]. Although appealing, the over stoichiometry mechanism raises the question of where these extra oxygens can be located in the structure (see Fig. 1). To answer this non trivial question, we have revisited the crystal chemistry of the chain-like oxides closely related to $Sr_4Mn_2CoO_9$ in the system Sr-Mn-Co-O. Starting from the generic formula $Sr_{1+x}(Mn_{1-x}Co_x)O_3$ characterized by the couple Mn^{4+}/Co^{2+} reported by previous authors [2, 30, 41-42], we have investigated how oxygen over stoichiometry may affect their structure during the synthesis in air. From single crystal , powder X-ray diffraction and high resolution electron microscopy (HREM) studies we show that the oxygen over stoichiometry mechanism plays a primordial role with a strong impact on their structure and chemistry and allows to form a large family of new aperiodic chain like structures $Sr_{1+x}(Mn_{1-x}Co_x)O_{3+\delta}$ in the domain $0.285 \leq x \leq 0.40$. We also demonstrate that for a fixed cationic composition, x=1/3, the aperiodic structure of $Sr_{4/3}(Mn_{2/3}Co_{1/3})O_{3+\delta}$ can be dramatically modified by a very small deviation from oxygen stoichiometry. It changes indeed continuously from the stoichiometric commensurate phase $Sr_4Mn_2CoO_9$ built up of only trimeric $M_2M'O_9$ units obtained for $\delta=0$ to an incommensurate oxide for $\delta=0.10$ which keeps the same cationic composition but whose structure consists of trimeric $M_2M'O_9$ and tetrameric $M_3M'O_{12}$ units.

Results and Discussion

Synthesis and characterization of a large family of aperiodic structures $Sr_{1+x}(Mn_{1-x}Co_x)O_{3+\delta}$: how to interpret the oxygen over stoichiometry mechanism?

Our investigation of the oxides $Sr_{1+x}(Mn_{1-x}Co_x)O_{3+\delta}$ is based on the different nature of the results that were previously obtained by two groups separately for a sample of identical nominal composition, $Sr_9Mn_5Co_2O_{21}$ [41-42]. For this composition, corresponding to x=2/7=0.2857 and δ= 0, Boulahya *et al* [41] obtained a commensurate structure **(Fig.1b)** which consists of the alternation of trimeric "Mn_2CoO_9"and tetrameric "Mn_3CoO_{12}" units. For the same nominal composition, similar times (7 days) and temperature (1200°C) of synthesis in air Battle et al [42] demonstrated an incommensurate structure from neutron powder diffraction data that was interpreted as having a cationic composition different from the nominal one. Although the two experimental methods were very similar they seem to differ by the cooling method that was involved, i.e. quenching at 1200°C for the commensurate phase [41] but was not indicated for the incommensurate oxide [42]. Bearing in mind that in cobalt-based oxides the presence of alkaline earth cations favors the partial oxidation of Co^{2+} into Co^{3+} [48], as recently invoked for the spin chain oxide $Sr_3CaMn_2CoO_{9+\delta}$ [45], this suggests that oxygen over stoichiometry should be the mechanism at play behind this different structural behavior. To unravel this intriguing problem of the actual localization of extra oxygen in these compounds, we have investigated a series of samples with the composition $Sr_{1+x}(Mn_{1-x}Co_x)O_{3+\delta}$, with x ranging from 0.2857 to 0.40 , all prepared in the same conditions at 1400°C in air and quenched at this temperature for the sake of comparison. The sample x=2/7 (0.2857) was chosen as a reference since it corresponds to the "nominal composition", $Sr_9Mn_5Co_2O_{21}$ which was obtained as a commensurate oxide by one of the previous authors [41]. The other x compositions were chosen as rational fractions (3/10, 5/16, 7/20, 6/17, 5/14, 4/11, 3/8 and 2/5) susceptible to produce commensurate spin chain oxides following a Farey tree hierarchy, i.e. $(Sr_4Mn_2CoO_9)_n.(Sr_5Mn_3CoO_{12})$ or $(Sr_4Mn_2CoO_9)_n.(Sr_3CoMnO_6)$ considering the possible absence of oxidation of Co^{2+} into Co^{3+} during the synthesis as will be discussed further.

All the investigated compositions allowed pure phases for $0.2857 \leq x \leq 0.40$ without any trace of impurity to be synthesized, with a structure closely related to that previously reported for $Sr_4Mn_2CoO_9$ [30] and $Sr_3CaMn_2CoO_9$[49]. This is exemplified by the powder X-ray diffraction (PXRD) patterns of the sample x=7/20 (**Fig. 2a**). However, only one pattern can be indexed in a hexagonal cell (a≈9.5 Å, c≈7.5 Å, space group P321) for the sample, x=3/8 showing a

commensurate structure. In contrast, all other patterns exhibit a shifting of several peaks (see **Fig. 2b-d**) which hinder their indexation in the latter cell and evidences incommensurability along *c*. Instead, the patterns could only be satisfactorily indexed using two *c* parameters, due to a misfit of periodicity between the Mn/Co chains ($c_1 \approx 2.56$-2.60 Å) and the Sr columns ($c_2 \approx 3.89$-3.99 Å). Thus, the aperiodic structure of all these oxides can be described in the super-space formalism using four cell parameters (a, a, c_1, c_2) and the modulation vector $q = \gamma c_1^*$, with $\gamma = c_1/c_2$. Then the PXRD patterns can be fully indexed with four *hklm* indices (**Fig. 2b-d**). The compositional and structural parameters are listed in **Table 1.**

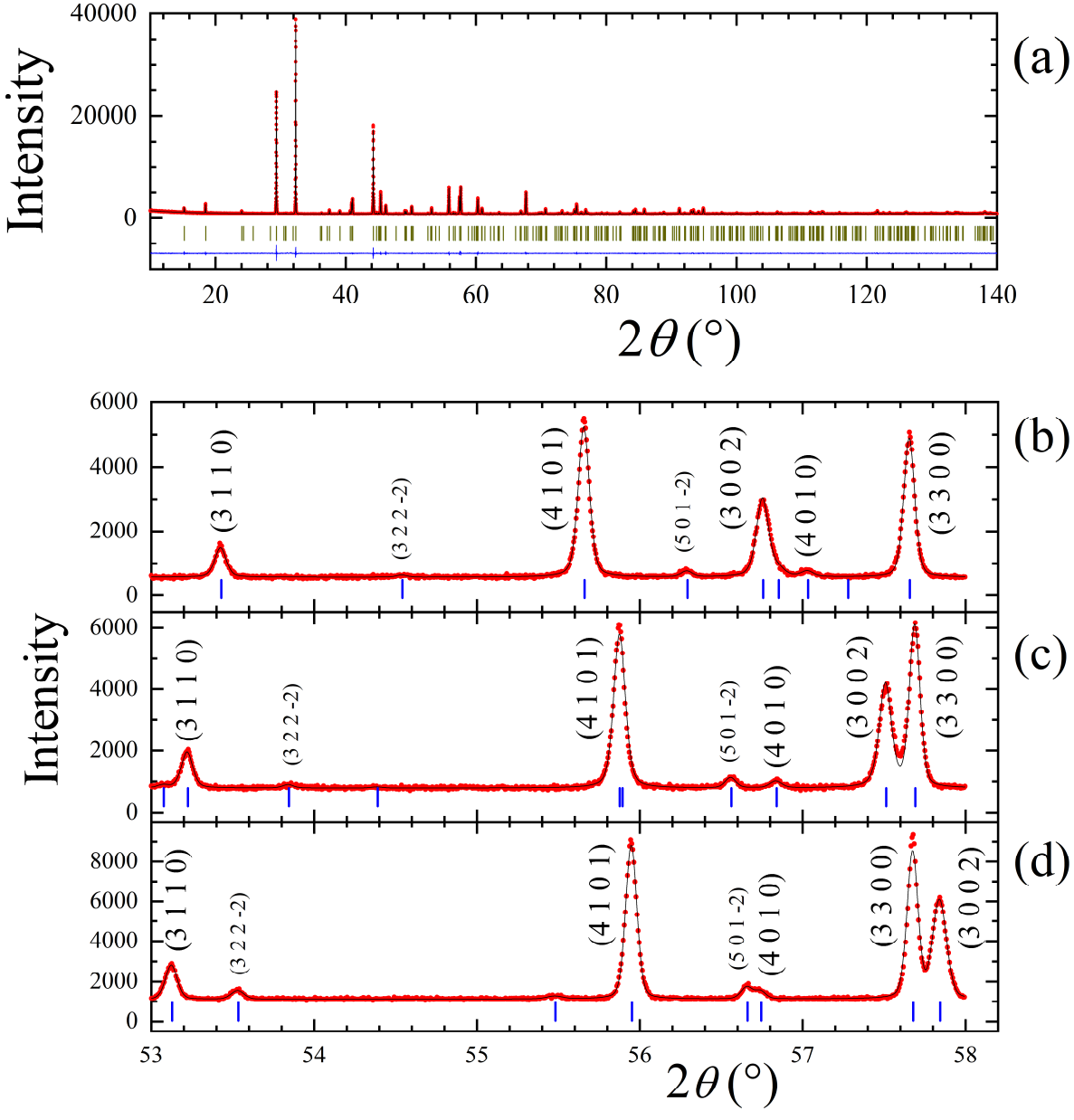

Fig.2 Powder X-Ray diffraction pattern of $Sr_{1+x}(Mn_{1-x}Co_x)O_{3+\delta}$ for x=7/20 (a) and part of PXRD patterns showing the shifting of main and satellite reflections for x=2/7 (b), x=7/20 (c) and x=3/8 (d).

Table1 Structural and compositional parameters of the chain oxides $Sr_{1+x}(Mn_{1-x}Co_x)O_{3+\delta}$, also formulated $Sr_{1+y}[(Mn_{1-x}Co_x)_{1-z}\square_z]O_3$. These oxides were synthesized in air up to 1400°C and quenched at this temperature.

$Sr_{1+x}(Mn_{1-x}Co_x)O_{3+\delta}$						**$Sr_{1+y}[(Mn_{1-x}Co_x)_{1-z}\square_z]O_3$**		
x		a	c_1	c_2	γ	y	z	δ
2/7	0.28571	9.5863(2)	2.5662(1)	3.9999(6)	0.6416(1)	0.2831	0.0020	0.0060
3/10	0.3	9.5824(2)	2.5728(2)	3.9846(7)	0.6457(1)	0.2914	0.0067	0.0201
5/16	0.3125	9.5852(3)	2.5721(2)	3.9776(9)	0.6466(1)	0.2933	0.0165	0.04461
7/20	0.35	9.5815(2)	2.5887(1)	3.9284(6)	0.6590(1)	0.3180	0.0237	0.0730
6/17	0.35294	9.5812(2)	2.5929(1)	3.9176(5)	0.6619(1)	0.3237	0.0216	0.0662
5/14	0.35714	9.5804(2)	2.5915(2)	3.9224(8)	0.6607(1)	0.3214	0.0263	0.0811
4/11	0.36364	9.5846(2)	2.5929(2)	3.9234(7)	0.6609(1)	0.3218	0.0307	0.0950
3/8	0.375	9.5850(2)	2.5983(3)	3.8977(12)	0.6666(1)	0.3332	0.0304	0.0940
2/5	0.4	9.5705(2)	2.6017(2)	3.8998(2)	0.6671(1)	0.3343	0.0469	0.1478

The evolution of the cell parameters versus the cobalt content x **(Fig.3)** though not perfectly regular shows a clear tendency. One observes that the *a* parameter is not significantly affected, with a mean value a ≈9.582(5) Å **(Fig.3a)**. This is in agreement with the fact that the inter-chain distances are before all governed by the size of the Sr^{2+} cations but not by the Sr content. The c_1 parameter which characterizes the "Mn,Co" sub-lattice tends to increase with x **(Fig.3b)**, while the c_2 parameter characteristic of the Sr sub-lattice tends to decrease as x increases **(Fig.3c)**.

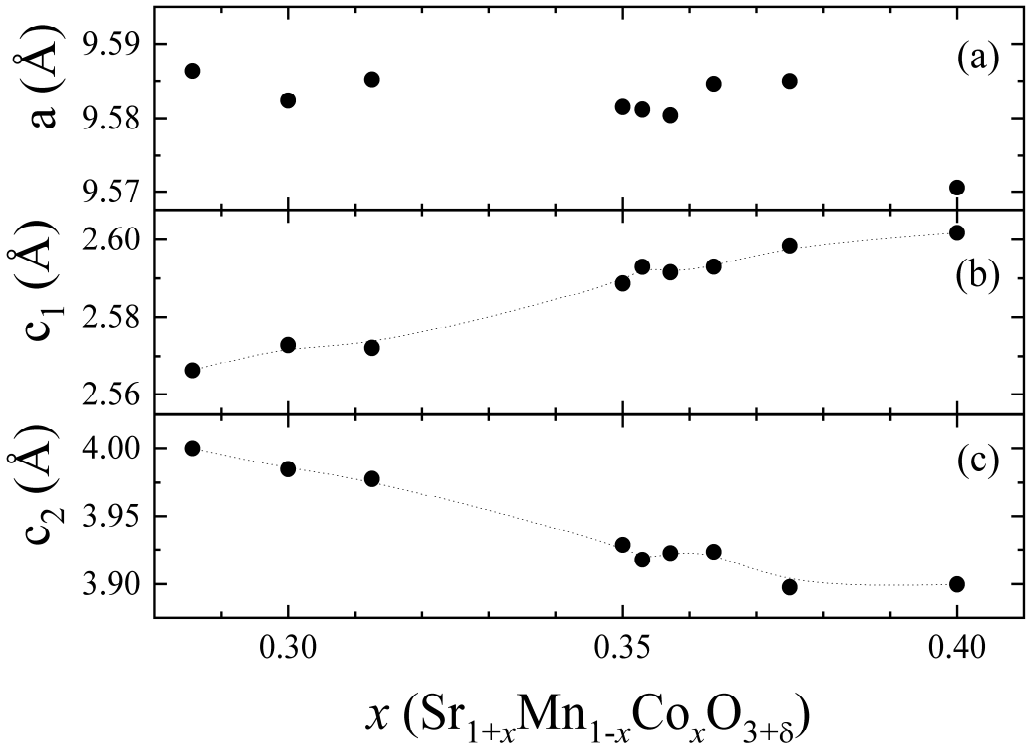

Fig.3 Evolution of the cell parameters of the oxides $Sr_{1+x}(Mn_{1-x}Co_x)O_{3+\delta}$ versus the cobalt content x.

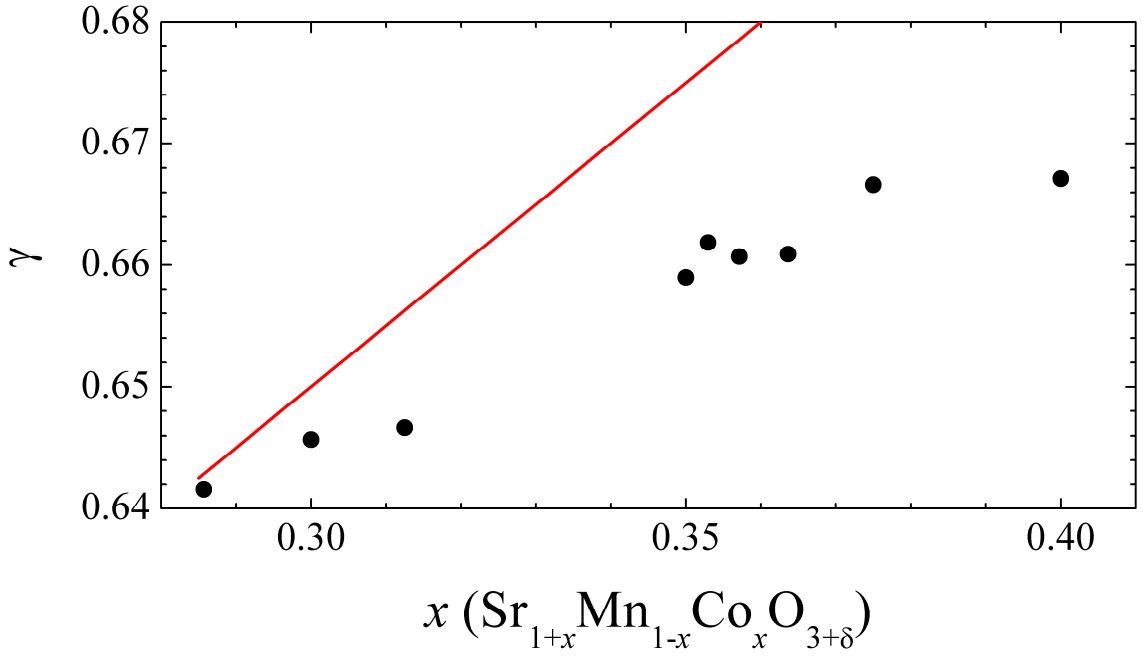

Fig.4 Evolution of the modulation vector γ versus the cobalt content x of the oxides $Sr_{1+x}(Mn_{1-x}Co_x)O_{3+\delta}$. The red line is the relationship between the composition x and the modulation vector γ_x expected for this composition: $\gamma_x = (x+1)/2$.

The $\gamma=c_1/c_2$ value which characterizes the structure modulation tends to increase with the cobalt content x **(Fig.4)**. At this point we have to consider the structural model previously reported by Perez-Mato *et al* [2] for the incommensurate hexagonal oxides $A_{1+x}(B_{1-x}A'_x)O_3$ related to the 2*H* hexagonal perovskites. From the nice model developed by these authors it was demonstrated that the modulation is simply linked to the x value by the relation $x = 2\gamma-1$, with $x= N_P/(N_P+N_O)$, where N_P and N_O represent the number of trigonal prisms and octahedra respectively in the polyhedral chains. Thus, for $Sr_{1+x}(Mn_{1-x}Co_x)O_3$ stoichiometric oxides obeying to the charge balance Mn^{4+}/Co^{2+}, a linear evolution of γ vs x should be expected according to this relation (see the red line **Fig.4**). From the comparison of the observed and theoretical evolution of γ vs x **(Fig.4)**, it clearly appears that the experimental behavior deviates significantly from the theoretical one. This deviation is an experimental evidence that the oxygen over stoichiometry mechanism previously proposed for $Sr_3CaMn_2CoO_{9+\delta}$ [45] influences dramatically the commensurability of these aperiodic structures. If one admits that the structure can hardly accommodate extra oxygen without any modification of the Co and Mn polyhedra, the only possibility left is to consider that the so formed oxides $Sr_{1+x}(Mn_{1-x}Co_x)O_{3+\delta}$ result in the presence of cationic vacancies, and must be reformulated as $Sr_{1+y}[(Mn_{1-x}Co_x)_{1-z}\square_z]O_3$. Considering this new formulation, extra oxygens can be incorporated in the chains during the synthesis through the formation of cation deficient polyhedra. As no secondary phase or impurity has been detected in any PXRD pattern of the different samples, we can consider that the cationic composition must be kept equal to the nominal composition. This statement is supported by the following features: (i) electron microscopy and SEM observations on many crystallites and grains do not detect any signature of an amorphous phase, (ii) the EDS analysis indicates that the cationic composition does not vary from one crystallite to the other, demonstrating a very high homogeneity of the samples, in agreement with the very narrow profile of the PXRD peaks. Thus we can write the following relations: $\frac{Co}{Mn} = \frac{x}{1-x}$ and $\frac{Sr}{Mn+Co} = \frac{1+x}{1} = \frac{1+y}{1-z}$.

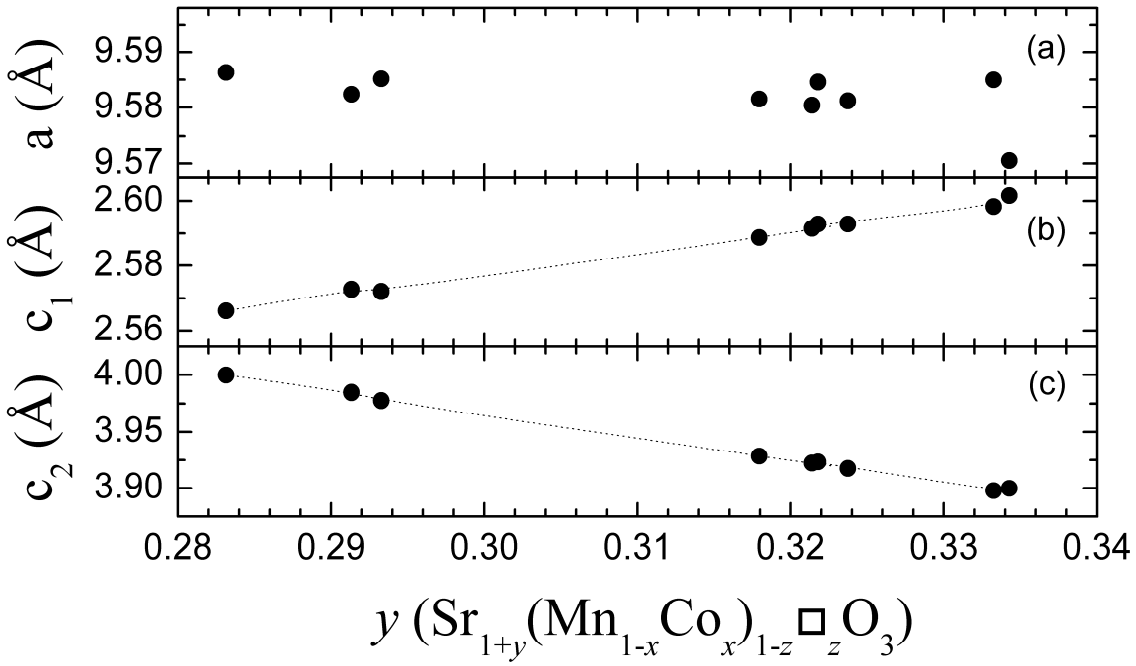

Fig.5 Evolution of the cell parameters versus y in the oxides $Sr_{1+y}[(Mn_{1-x}Co_x)_{1-z}\square_z]O_3$.

The vacancy rate z is then determined by the relation z=(x-y)/(1+x) in order to respect the nominal cationic composition. Therefore, in those oxides, y = $N_P/(N_P+N_O)$ and can be obtained from the relation y =2γ-1 (**Table 1**) through the PXRD indexation (γ= c_1/c_2). The oxygen uptake δ (**Table1**) can then be deduced from the equivalence of the two formula, $Sr_{1+x}(Mn_{1-x}Co_x)O_{3+\delta}$ and $Sr_{1+y}[(Mn_{1-x}Co_x)_{1-z}\square_z]O_3$, by the relation: δ=3(x-y)/(1+y).

The evolution of the cell parameters vs *y* (**Fig.5**) is practically linear for most of the compositions, i.e. c_1 increases with y (**Fig.5b**), while c_2 decreases as *y* increases (**Fig.5c**). Note that for some compositions a deviation from the linear evolution is observed. This feature will be shown further to be due to the high sensitivity of the structural parameters of these oxides to the oxygen stoichiometry and consequently to the temperature gradient inside the furnace during synthesis.

Evidence for cationic vacancies on trigonal prismatic sites: Commensurate structure of the oxide $Sr_{11/8}(Mn_{5/8}Co_{3/8})O_{3+\delta}$ (δ≈0.094).

The oxygen over stoichiometry mechanism that we propose here is based on the existence of cationic vacancies in the polyhedral chains, a feature that has never been reported before in Mn/Co based spin chain oxides. In order to shed light on this issue, we have focused our attention on the commensurate oxide x=3/8, which exhibits a γ value of 2/3 like $Sr_4Mn_2CoO_9$ reported by Boulahya et al [30] in spite of its different cationic composition compared to the latter (x=1/3). For this purpose, single crystals of this compound were extracted from the batch obtained for the synthesis

of the polycrystalline sample for a structural study. The detailed structure determination of this phase from a single crystal labeled **crystal 1** is reported in supplemental information SI1. It was carried out independently in the superspace formalism and in the normal hexagonal supercell (*a, a, 3c1*) in agreement with its commensurate character. The second method allows advantageously the two different types of polyhedral "Mn_2Co"chains to be distinguished. The cell parameters observed for the single crystal close to those of the polycrystalline sample indicate that the latter is homogeneous and that the composition of the single crystal is representative of the bulk. Nevertheless, as expected, the obtained parameters are still close to those observed by Boulahya et al [30] for $Sr_4Mn_2CoO_9$ (x=1/3), as summarized in **Table 2**. Single crystal refinements were then carried out in the hexagonal commensurate "*a*, *c*" cell from 2478 reflections for 13 crystallographic sites (3 Sr, 3 Mn, 2 Co, 5 O sites), bearing in mind that the latter cannot allow to determine the distribution of cobalt and manganese and the Mn /Co ratio due to the too close atomic numbers of these elements (Z_{Mn}=25, Z_{Co}=27). A first cycle of refinements performed for a full occupancy of the Mn and Co sites according to the formula $Sr_{4/3}(Mn_{2/3}Co_{1/3})O_3$ as previously reported for $Sr_4Mn_2CoO_9$ [30] led to an agreement factor R=0.054. At this point of the investigation, we took into consideration our chemical results which impose that the cationic Mn/Co ratio, is not 2 as for $Sr_{4/3}(Mn_{2/3}Co_{1/3})O_3$ but 1.666 as observed for $Sr_{1.375}(Mn_{0.625}Co_{0.375})O_{3+\delta}$ (Table 1). Therefore attempts to refine the structure for the composition "$Sr_{4/3}(Mn_{0.625}Co_{0.375})O_3$" were performed, which did not change significantly the R factor, as expected. In contrast, the refinement of the occupancy factors of the two trigonal prismatic sites, Co1 and Co2, showed a significant decrease of the R factor from 0.054 to 0.0374 due to a 20% decrease of the Co2-site occupancy, whereas the Co1 site was only showing 5% of vacancy. The atomic parameters refined in the (3+1)D approach and in the supercell approach are detailed in supplemental information (**Tables SI-2** and **SI-3** respectively). These refinements lead to the ultimate structural formula $Sr_{4/3}(Mn_{0.606}Co_{0.364}\square_{0.03})O_3$, whose cationic composition coincides practically with the nominal composition $Sr_{1.375}(Mn0.625Co_{0.375})O_{3+\delta}$ (**Table 1**). Thus, these results demonstrate that due to oxygen over-stoichiometry a new commensurate $Sr_4Mn_2CoO_9$-type oxide, with the formula $Sr_4(Mn_{1.818}Co_{1.092}\square_{0.09})O_9$ corresponding to a significantly smaller Mn/Co ratio has been synthesized. Quite remarkably, the trimeric polyhedral units of this phase **(Fig.6)** differ from the stoichiometric $Sr_4Mn_2CoO_9$ **(Fig.1a)**, by the presence of cationic vacancies on the trigonal prismatic sites, implying that Co^{2+} has been partially oxidized into Co^{3+} according to the formal charge balance $Sr_4(Mn^{IV}_{1.818}Co^{III}_{0.544}\ Co^{II}_{0.548}\square_{0.09})O_9$. In this structure, the octahedral sites are fully occupied by manganese and cobalt, most probably distributed at random, whereas the trigonal prismatic sites are exclusively occupied by cobalt. Considering that the trigonal prismatic sites

Co1 and Co2 belong to two different rows of polyhedra labeled A and B, this structure (**Fig.6**), can be described as the ordered assemblage of "trigonal prismatic Co-deficient" B-rows [$Mn_{1.818}Co_{1.047}\square_{0.135}O_9$] (proportion: 2/3) and fully occupied A-rows [$Mn_{1.818}Co_{1.182}O_9$] (proportion: 1/3). The analysis of the M-M' and M-M interatomic distances along *c* (Fig. 6b) shows that the M-M distances between two nearest Oh sites (mainly occupied by Mn^{4+}) are rather similar in A and B chains ranging from 2.554 to 2.570 Å, respectively. The M-M' distances between two neighboring Oh/Tp sites show that the cobalt cation of the Tp sites of the B chains is significantly off centered , with two different M-Co-M distances of 2.581 and 2.655 Å along *c*, compared to the A chains where Co is in symmetric position with two Co-M distances of 2.626 Å. The inter atomic distances M-M, M-M', M-O, M'-O along c, as well as the O-O distances of the trigonal prismatic sites parallel to *c* are detailed in supplemental information (**Tables SI-5** and **SI-6**).

Table 2 Crystal parameters of the commensurate oxide $Sr_{1+x}(Mn_{1-x}Co_x)O_{3+\delta}$ for x=3/8 (single crystal and polycrystalline powder) compared to commensurate $Sr_4Mn_2CoO_9$ (x=1/3) oxide obtained by Boulahya et al [30].

	a (Å)	c_1 (Å)	c_2 (Å)	γ	c (Å)
Single crystal	9.5878(2)	2.602(1)	3.9029(1)	2/3	7.8058(2)
Polycrystal	9.5850(2)	2.5983(3)	3.8977(4)	2/3	7.7954(8)
Polycrystal[30]	9.5852(7)	2.6088(2)	3.9133(2)	2/3	7.8266(4)

This structural study strongly supports the underlying oxygen over stoichiometry mechanism. Considering the generic formula $Sr_{1+y}[(Mn_{1-x}Co_x)_{1-z}\square_z]O_3$, the rate of cationic vacancies calculated from this model, z=0.0304 for the commensurate oxide "x=0.375, y=1/3" (see **Table 1**) is equal to the observed value obtained from the single crystal study of this oxide, $Sr_{4/3}(Mn_{0.606}Co_{0.364}\square_{0.03})O_3$. Thus, from the oxides $Sr_{1+y}[(Mn_{1-x}Co_x)_{1-z}\square_z]O_3$ listed in **Table 1**, it appears that for the given conditions of synthesis (at 1400°C in air followed by quenching) all of them exhibit cationic vacancies on the prismatic Co sites and that the vacancy rate z tends to increase with the cobalt content from z≈0.002 for x=0.28571 to z≈0.03 for x=0.375.

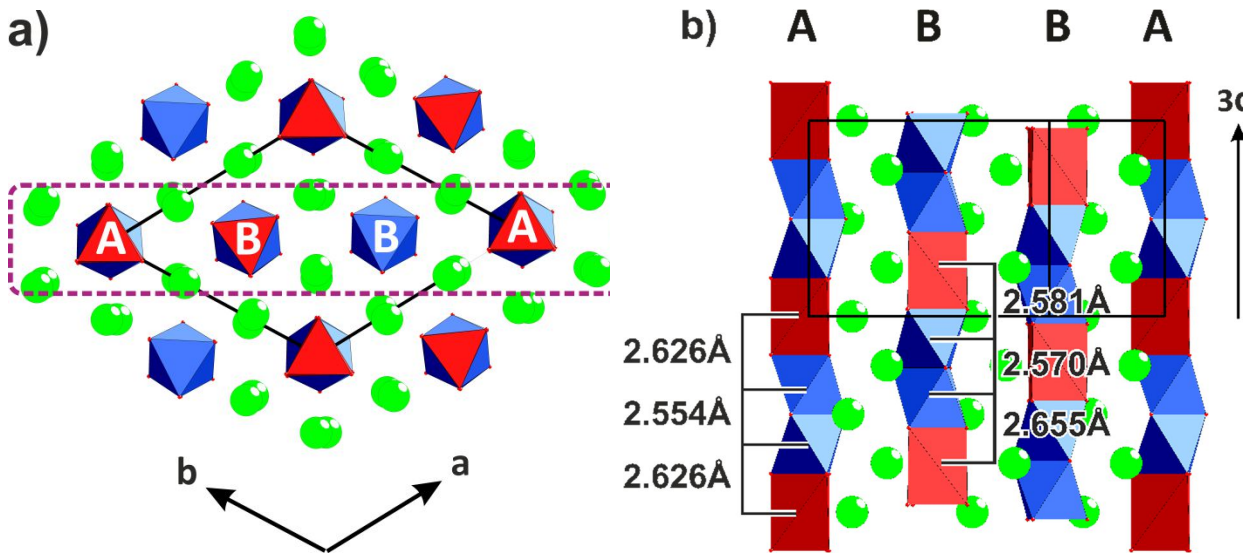

Fig.6 Structure of the commensurate oxide $Sr_{4/3}(Mn_{0.606}Co_{0.364}\square_{0.03})O_3$ (crystal I) : (a) projection onto the (001) plane, (b) projection along [120] of the slab enlightened by the violet dashed line rectangle in Fig.6a. Two sorts of polyhedral A and B chains are shown. The M-M and M-M' interatomic distances between the MO_6 octahedra and the $M'O_6$ prisms along c are reported.

Note that the lowest vacancy content is observed for the reference sample x=2/7 (0.28571). We find that this sample is incommensurate, as reported by Battle et al [42], but with a γ value of 0.64157 intermediate between that obtained by these authors (0.64024) and the value observed by Boulahya et al [41] for the same cationic composition but with a commensurate structure, which implies a γ value of 0.64286. This clearly indicates that the commensurability of the structure and consequently the cationic vacancy content z is highly sensitive to the nature of the thermal treatment in air. Correlatively, the extra oxygen content δ (**Table 1**) with respect to the stoichiometric formula $Sr_{1+x}(Mn_{1-x}Co_x)O_3$, increases with x, from δ ≈0.006 for x=0.2857 to δ ≈0.094 for x=0.375. The quasi linear evolution of the oxygen uptake δ versus x in those oxides (**Fig.7**) shows the primordial role of the cobalt content in the oxygen over-stoichiometry mechanism, due to the partial oxidation in air of Co^{2+} into Co^{3+}. The difficulty for obtaining a perfectly continuous and reproducible evolution of "z, δ" is easily explained by the fact that the extra oxygen content in these materials is highly sensitive to the oxygen pressure during the synthesis, and may vary slightly from one experiment to the other due to slight fluctuations of temperature during synthesis and cooling.

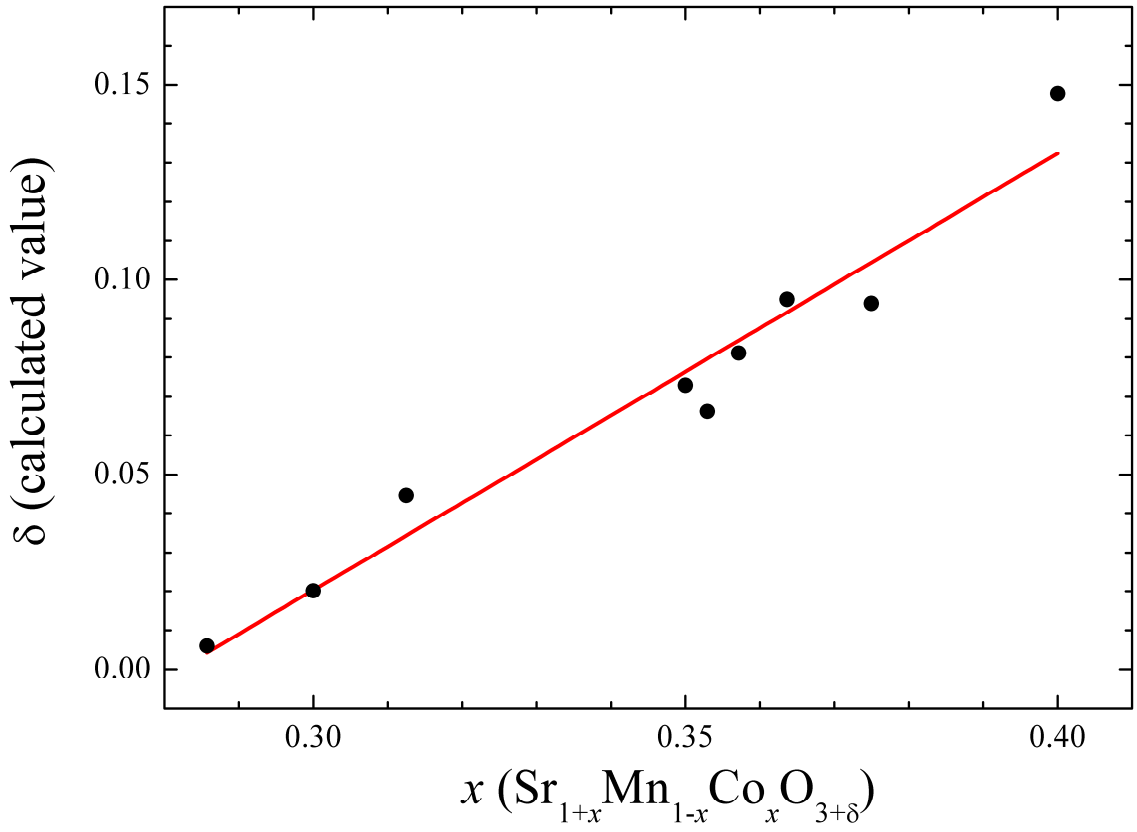

Fig.7 Evolution of the oxygen over-stoichiometry δ versus the cobalt content in the oxides $Sr_{1+x}(Mn_{1-x}Co_x)O_{3+\delta}$

Effect of synthesis conditions on oxygen over stoichiometry: new aperiodic structures $Sr_{4/3}(Mn_{2/3}Co_{1/3})O_{3+\delta}$

Bearing in mind that these oxides are highly sensitive to the oxygen pressure, it can be expected that for a fixed cationic composition their oxygen stoichiometry and consequently their aperiodic structure will deeply depend on the synthesis conditions (temperature, gaseous atmosphere, cooling method, etc…). Based on these results, we have studied in a last step the oxygen non-stoichiometry for a fixed cationic composition, in the system $Sr_{4/3}(Mn_{2/3}Co_{1/3})O_{3+\delta}$ which corresponds to extra oxygen incorporation with respect to the prototype $Sr_4Mn_2CoO_9$ (δ=0) oxide, discovered by Boulahya et al [30].

Different samples with the same nominal cationic composition "$Sr_{4/3}Mn_{2/3}Co_{1/3}$"were synthesized in various experimental conditions, in order to understand the impact of oxygen non-stoichiometry upon the structural nature of the oxide $Sr_{4/3}(Mn_{2/3}Co_{1/3})O_{3+\delta}$. The structural parameters for six different samples are listed in **Table 3**.

Table 3: Structural parameters of the oxides $Sr_{4/3}Mn_{2/3}Co_{1/3}O_{3+\delta}$, also formulated $Sr_{1+y}[(Mn_{2/3}Co_{1/3})_{1-z}\square_z]O_3$.

	$Sr_{4/3}Mn_{2/3}Co_{1/3}O_{3+\delta}$			$Sr_{1+y}[(Mn_{2/3}Co_{1/3})_{1-z}\square_z]O_3$		
Synthesis Conditions	a	c_1	γ	y	z	δ
Pristine (1250 °C)	9.5916(2)	2.5756(1)	0.6510(1)	0.3020	0.0235	0.0721
Annealed-Air A-Air (1425 °C)	9.5883(5)	2.5845(2)	0.6554(2)	0.3109	0.0168	0.0514
Crystals-Air "Crystal II" (1500 °C)	9.5968(14)	2.5904(10)	0.6596(10)	0.3193	0.0105	0.0320
Annealed-Argon "A-Ar1" (1375 °C)	9.5936(2)	2.5907(1)	0.6619(1)	0.3237	0.0072	0.0218
Annealed-Argon "A-Ar2" (1420 °C)	9.5945(4)	2.5963(3)	0.6648(3)	0.3295	0.0029	0.0086
Sealed tube "ST" (1150 °C)	9.5825(6)	2.5959(5)	2/3	1/3	0	0

For a protocol involving several steps in the synthesis of the precursor described in the experimental section a first sample finally sintered at 1250°C labeled as pristine P-1250 is prepared, with an incommensurate structure (γ = 0.6510) indicating significant oxygen excess (δ=0.0721) and cation deficiency (z=0.0235). Then it is observed that by annealing the sample P-1250 at higher temperature either in air (A-air1425) or in argon (A-Ar1375) the γ value is significantly increased up to 0.6555 and 0.6619 showing that the δ value is decreased to 0.05 and 0.02 respectively due to oxygen departure. This effect of temperature and atmosphere is corroborated by the growth of single crystals in air at higher temperature (1500°C) allowing a γ value of 0.6590 larger than that of the A-air1425 sample but smaller than for the A-Ar-1375 sample. In the same way, annealing a sample under an argon flow at higher temperature 1420°C (Ar-1420) allows still a higher γ value of 0.6648 to be reached corresponding to a very small oxygen excess, δ≈0.009. Finally, we succeeded to synthesize the commensurate stoichiometric oxide $Sr_4Mn_2CoO_9$ (γ =2/3, δ=0) from a stoichiometric mixture of the oxides SrO, MnO_2, Co_3O_4 with metallic cobalt heated at 1150°C in sealed tube (sample ST-1150).

These results show that it is possible to synthesize a series of incommensurate oxides with the same cationic composition $Sr_{4/3}(Mn_{2/3}Co_{1/3})O_{3+\delta}$ by carefully controlling the oxygen stoichiometry during the synthesis. They demonstrate that for a fixed cobalt content, the extra oxygen stoichiometry δ, which corresponds to the partial oxidation of Co^{2+} into Co^{3+} governs the aperiodic

character of the structure, γ increasing as δ decreases (**Table 3**). The cell parameters c_1 and c_2 of these $Sr_{4/3}(Mn_{2/3}Co_{1/3})O_{3+\delta}$ oxides show a linear evolution vs *y* (**Fig.8**) on the basis of

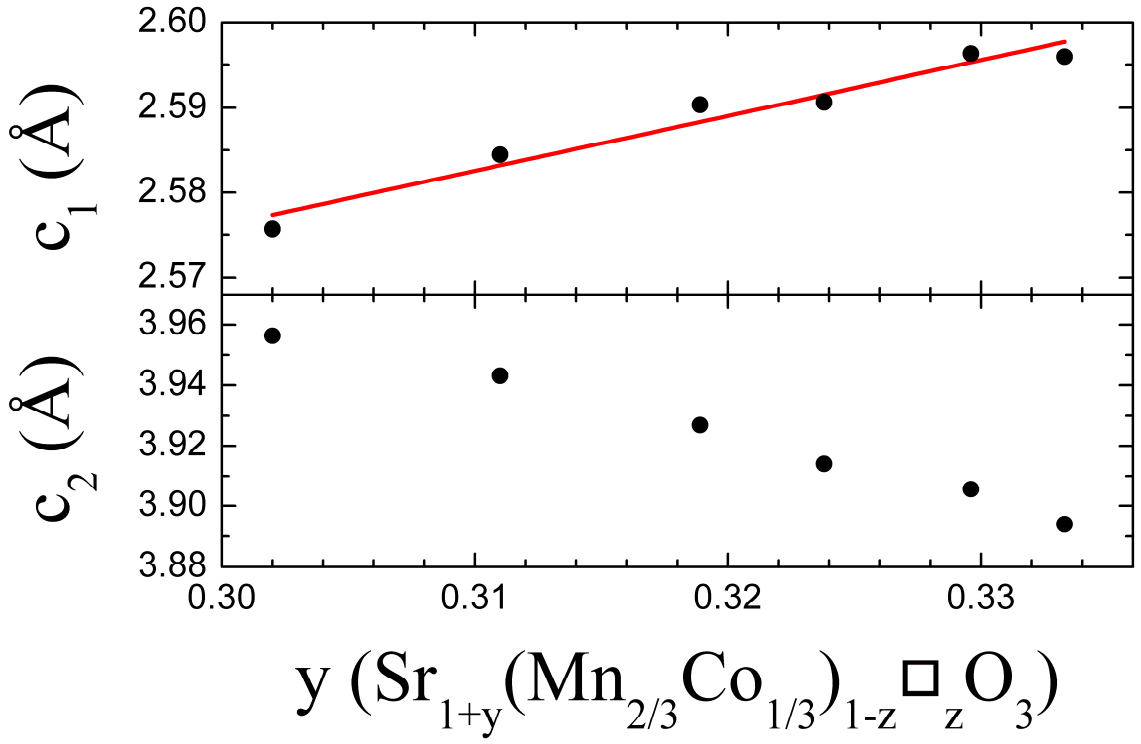

Fig.8 Evolution of the cell parameters of the oxides $Sr_{1+y}[(Mn_{2/3}Co_{1/3})_{1-z}\square_z]O_3$ versus y

the formula $Sr_{1+y}[(Mn_{2/3}Co_{1/3})_{1-z}\square_z]O_3$, confirming the prominent role of oxygen incorporation in the incommensurability of these oxides. Therefore, it is clearly observed that the proportion of prismatic trigonal sites with respect to octahedral sites, $y=N_P/(N_P+N_O)$ decreases as the rate of cationic vacancies z and the oxygen excess δ increase (**Table 3**).

In order to support this oxygen over-stoichiometry mechanism single crystals were grown at 1500°C (sample crystal II in Table 3) for structure investigation. The aperiodic structure of those crystals revealed a γ value of 0.659(1), identical to that observed from PXRD (Table 3). The structure determination of this oxide was carried out in the superspace approach. Details of the refinement are proposed in supplemental information **SI-1**. The final structural model is closely related to the structure of $Sr_{11/8}(Mn_{5/8}Co_{3/8})O_{3+\delta}$ (δ~0.09) in the (3+1)D treatment. Nevertheless, the refinement did not allow a significant amount of cationic vacancies on the prismatic sites to be evidenced (see refined atomic parameters of this crystal in **Table SI-4**). Such a feature is easily explained by the fact that the superspace approach is not very sensitive to such a phenomenon (see refinement of $Sr_{11/8}(Mn_{5/8}Co_{3/8})O_{3+}\delta$ in supplemental information **SI-1**) and that the expected

proportion of vacancies (z=0.01 in Table 3) is much lower than for $Sr_{11/8}(Mn_{5/8}Co_{3/8})O_{3+\delta}$ (z= 0.03 in Table 1). In contrast, this refinement clearly establishes the presence of tetrameric $M_3M'O_{12}$ units among a majority of trimeric $M_2M'O_9$ units, in agreement with the deviation of γ from 2/3.

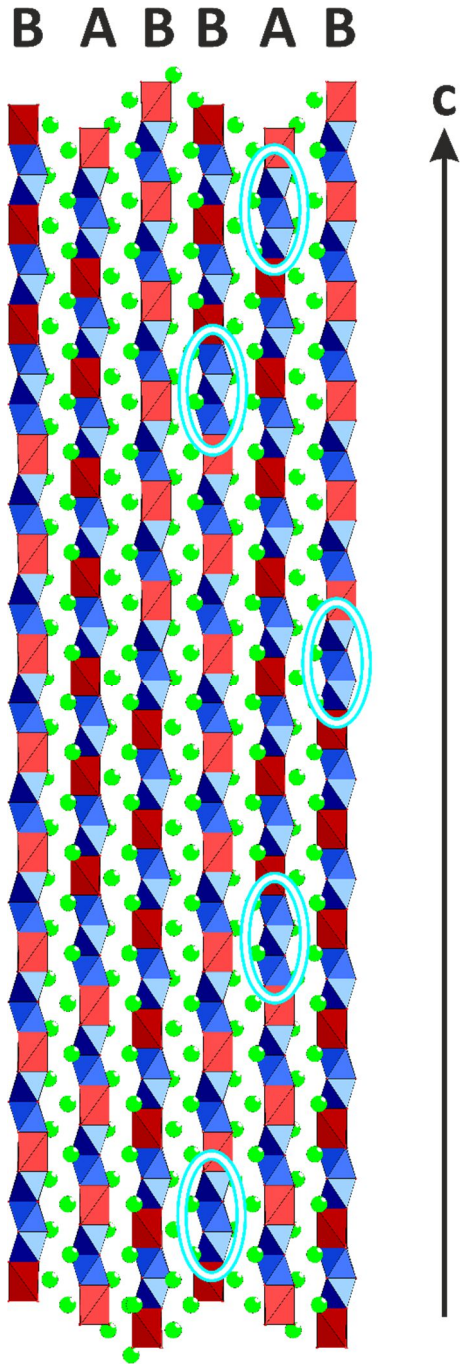

Fig. 9: Projection along the [1 2 0] direction of 6 prism–octahedra columns (BABBAB) depicted in the figure 6 for the crystals II. Sequences of three successive Oh are cyan circled.

Fig. 9 evidences the tetrameric units extracted from the Crystal II data; in this sample the $M_3M'O_{12}$ unit is repeated approximately every 7 motifs. The evolution of the metal–metal distances in the A or B chains of this incommensurate composite crystal is summarized in **Fig. 10**, versus the t parameter (internal parameter in the superspace description related to the 4^{th} dimension). Note that,

due the composite nature of the crystal, the structure resolution does not allow to differentiate the A and B chains, which appear as equivalent. Three different zones labeled 1 to 3 can be identified for characterizing the M-M and M-M' interatomic distances along the chains. In the zone 1 which represents the trimeric Oh_2Tp groups of the trimeric $M_2M'O_9$ units the M-M' distances between the Oh octahedral and the Tp prismatic site vary significantly from 2.57 Å to 2.60 Å, while the M-M distances between two octahedral sites are rather constant around 2.55 Å. In the zone 2 which corresponds to the tri-octahedral $(Oh)_3$ groups belonging to the tetrameric $M_3M'O_{12}$ units, the M-M distances between two octahedral sites are very homogeneous and do not vary significantly, remaining close to 2.56 Å. In contrast, the zone 3, which represents the groups (Oh)Tp(Oh) "bridging" either two $M_2M'O_9$ or one $M_2M'O_9$ to one $M_3M'O_{12}$ unit exhibit a strong variation of the M-M' versus t from 2.57 to 2.60 Å. Moreover, the M-M' distances are highly dissymmetric, i.e. the M' cation is off centered inside the Tp prism toward the $M_3M'O_{12}$ or $M_2M'O_9$ unit. The inter atomic distances, M-M',M-M, M-O and M'-O along *c* as well as the O-O distances of the $M'O_6$ trigonal prisms parallel to *c* are detailed in **Tables SI-5**.and **SI-6.**

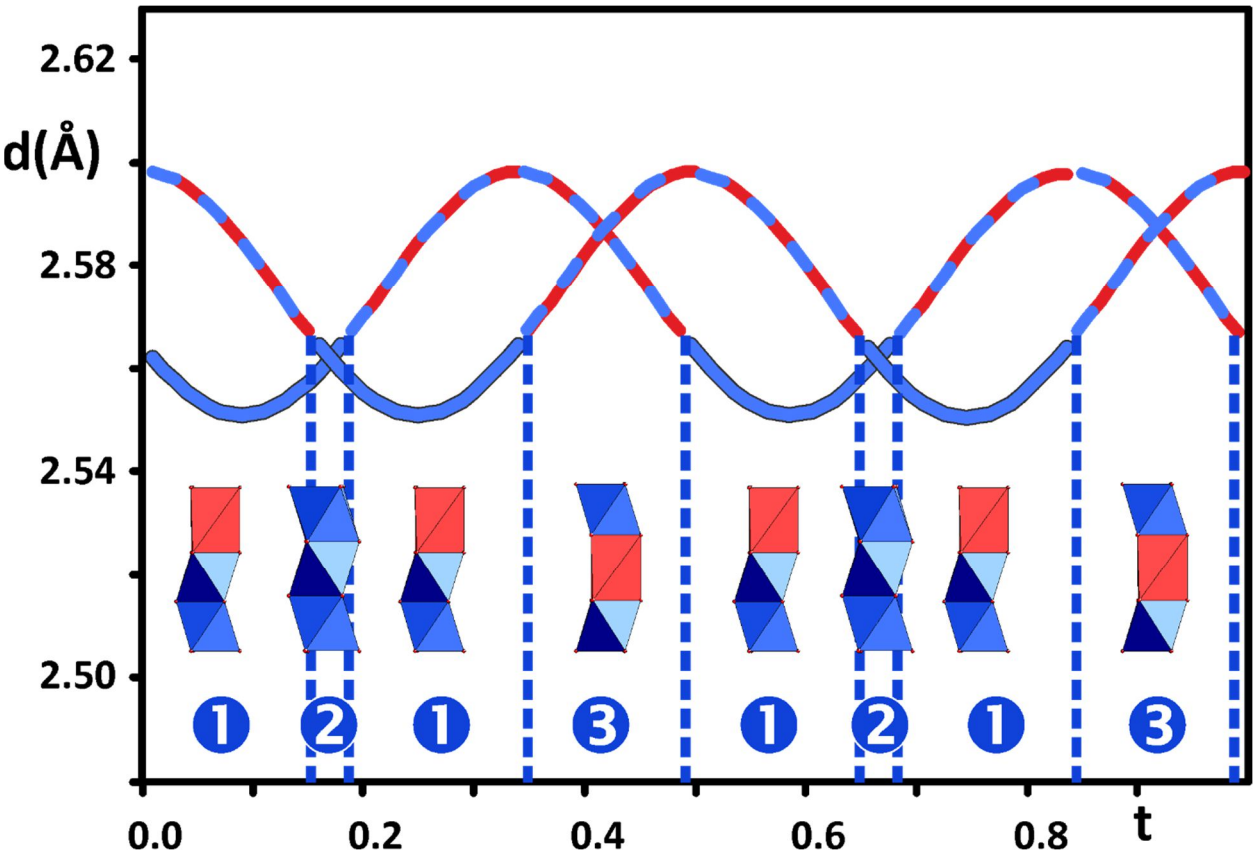

Fig. 10: Distances between M and M' sites along c for the incommensurate crystal of sample Crystal II : Evolution versus the internal t parameter of the M–M (blue curves) and M–M' (dashed red – blue curves) distances for three metallic first neighbors within A or B chains. Three different

areas are identified depending on the observed distances; a parallel analysis of the figure 9 makes it possible to assign each zone to the relevant building units. Zone 1: M–M and M–M' distances for a $M_2M'O_9$ unit. Zone 2: M–M distances for $(Oh)_3$ groups belonging to $M_3M'O_{12}$units Zone 3: M'–M' distances for "OhTpOh" groups bridging two $M_2M'O_9$ units or one $M_2M'O_9$ and one $M_3M'O_{12}$unit.

Influence of cobalt content and oxygen stoichiometry on the coexistence of two types of structural units in the oxides $Sr_{1+x}(Mn_{1-x}Co_x)O_{3+\delta}$

From the above results, it appears that the polyhedral chains of these oxides are generally built up of two sorts of structural units, either trimeric "$M_2M'O_9$"(2 octahedra +1 trigonal prism) and tetrameric "$M_3M'O_{12}$"(3 octahedra +1 trigonal prism) units or of trimeric and dimeric "$MM'O_6$"(1 octahedron +1 trigonal prism) units. The commensurate $Sr_4Mn_2CoO_9$ compound is built from the regular stacking of trimeric units only. This can be evidenced using high resolution electron microscopy (HREM) images taken along a direction perpendicular to the stacking direction. In Fig. 11a, where a [3-10] direction is selected, a regular stacking is observed in agreement with the simulated image Fig. 11b based on the structure refined from single crystal x-ray diffraction (crystal 1 in Supplementary Information). The commensurate nature of this compound is also confirmed by selected area electron diffraction (SAED) Fig. 11c where no spots splitting can be observed along the c* direction. As the γ value deviates from 2/3, the appearance of tetrameric units is signed by a modification of the previously observed regular stacking as illustrated Fig. 11d. The existence of an incommensurate ordering is revealed in SAED patterns by the splitting of some spots along the c* direction (Fig. 11e).

Thus, these oxides can be represented by the formula $[Sr_4M_2M'O_9]_{1-\alpha}$ $[Sr_5M_3M'O_{12}]_\alpha$ or $[Sr_4M_2M'O_9]_{1-\alpha}[Sr_3MM'O_6]_\alpha$ depending on the cationic composition *y,* where M and M' represent the octahedral and trigonal prismatic sites respectively, containing various contents of cationic species (Mn^{4+}, Co^{2+}, Co^{3+}) and vacancies (□). Considering that y determines the proportion of trigonal prismatic sites (N_P) and octahedral sites (N_O) according to the formula $y= N_P/(N_P+N_O)$, one can calculate the proportion of those units. The latter is characterized by the α or α' value which represents the fraction of tetrameric or dimeric units respectively which coexist with trimeric units. It can be obtained from the relations α=(1-3y)/y for the mixed chains built up of trimeric and tetrameric units and α'= (3y-1)/y for the mixed chains built up of trimeric and dimeric units.

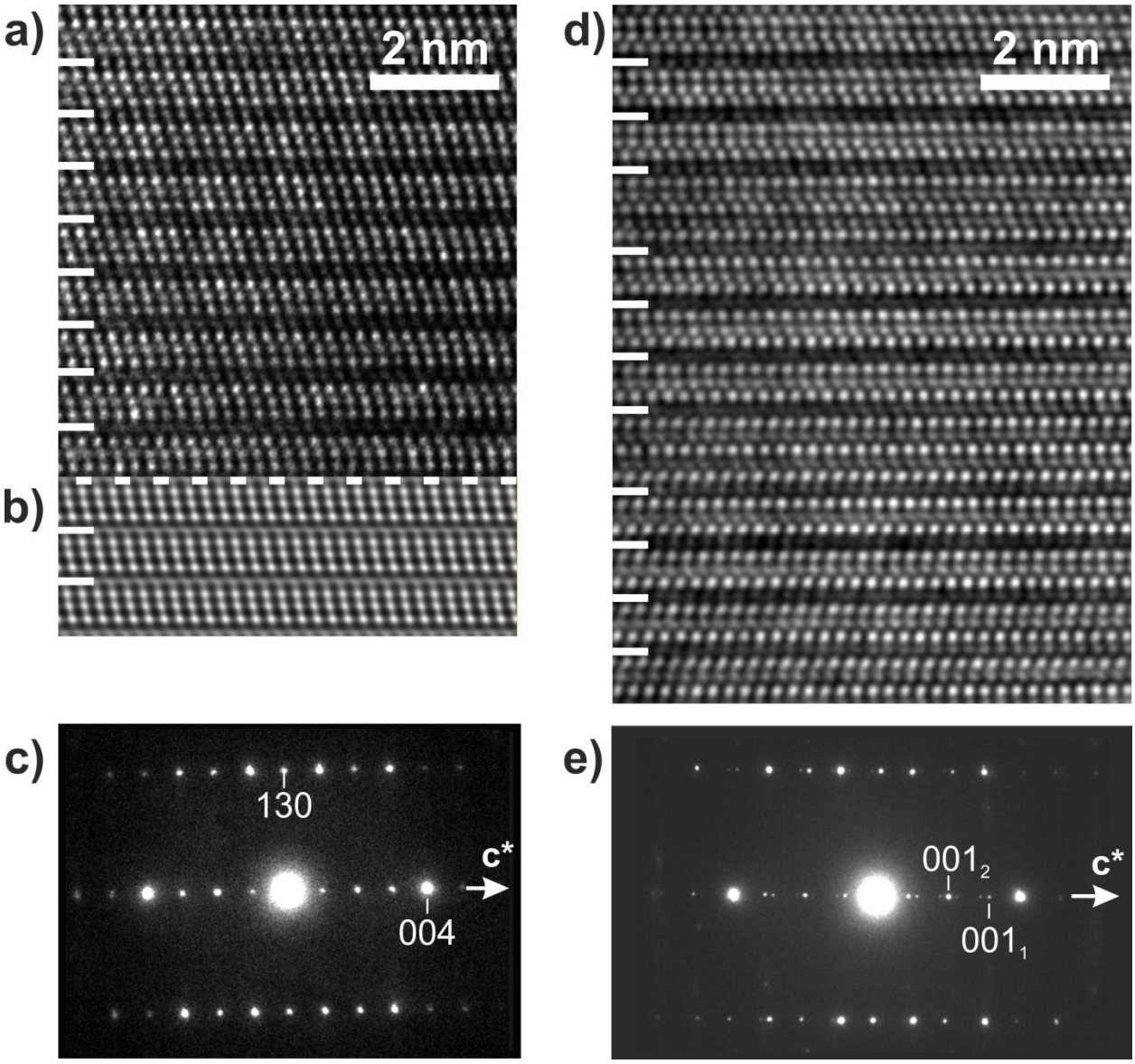

Fig. 11: Transmission electron microscopy observation along the [3-10] direction of two members of the $Sr_{1+x}(Mn_{1-x}Co_x)O_{3+\delta}$ compounds. In a) HREM image, b) HREM image simulation (thickness 17.3 nm, defocus 75 nm) and c) SAED patterns for $\gamma=2/3$. In d) HREM image and e) SAED patterns for $\gamma\approx0.64$.

Table 4 : Proportion of tetrameric units with respect to trimeric units α, extra oxygen content δ and Co^{3+} content in oxides $Sr_{4/3}(Mn_{2/3}Co_{1/3})O_{3+\delta}$ oxides also formulated $Sr_{1+y}[(Mn_{2/3}Co_{1/3})_{1-z}\square_z]O_3$.

y	α	δ	$nCo^{3+}=2\delta$
0.3020	0.3113	0.0722	0.1444
0.3109	0.2165	0.0513	0.1027
0.3193	0.1319	0.0319	0.0638
0.3237	0.0893	0.0218	0.0437
0.3295	0.0349	0.0086	0.0173
1/3	0	0	0

The evolution of the α value versus δ observed for the oxides $Sr_{4/3}Mn_{2/3}Co_{1/3}O_{3+\delta}$, which are characterized by a fixed cationic composition (**Table 4**) clearly shows that the extra oxygen incorporation alone influences dramatically the structure of these oxides. One indeed observes that the tetrameric units are absent (α=0) in the stoichiometric oxide (δ=0) and that their proportion increases with δ up to more than 31% for δ≈0.072. It should also be noted that correlatively the proportion of Co^{3+} in the polyhedral chains increases dramatically with δ from 0% in the stoichiometric oxide (δ=0) which contains $Mn^{4+}$and Co^{2+} exclusively to ≈ 43% of the total Co content for δ≈0.072. These results demonstrate that the oxygen over stoichiometry has to be carefully controlled and determined on the samples of these oxides in order to understand and to interpret their magnetic properties.

Table 5 : Proportion of tetrameric (or dimeric) with respect to trimeric units α, extra oxygen content δ and Co^{3+} content in $Sr_{1+x}(Mn_{1-x}Co_x)O_{3+\delta}$ oxides also formulated $Sr_{1+y}[(Mn_{1-x}Co_x)_{1-z}\square_z]O_3$. These oxides were synthesized in air up to 1400°c and quenched at this temperature

$[Sr_4M_2M'O_9]_{1-\alpha}\ [Sr_5M_3M'O_{12}]_\alpha$				
x	y	α	δ	n Co^{3+}= 2 δ
0.2857	0.2831	0.532	0.006	0.012
0.30	0.2914	0.432	0.020	0.040
0.3125	0.2933	0.409	0.045	0.089
0.350	0.3180	0.145	0.073	0.146
0.35294	0.3237	0.089	0.066	0.133
0.35714	0.3214	0.111	0.081	0.162
0.36364	0.3218	0.108	0.095	0.190
0.375	0.3332	0	0.094	0.188
$[Sr_4M_2M'O_9]_{1-\alpha'}[Sr_3MM'O_6]_{\alpha'}$				
x	y	α'	δ	n Co^{3+}= 2 δ
0.4	0.3343	0.008	0.143	0.296

The α values obtained for various cobalt contents in the samples quenched at 1400°C are listed in **Table 5.** It can be seen that for 0.2857 ≤ x < 0.375 the two sorts of trimeric "$M_2M'O_9$"and tetrameric "$M_3M'O_{12}$" units coexist within the chains, with an aperiodic distribution. Moreover, the fraction α of tetrameric units tends to decrease as the cobalt content x increases from more than 50% for x=0.2857 to 0% for x=0.375 which exhibits trimeric units exclusively. This evolution is due to the combined effect of the variation of the cationic Co/Mn ratio and of the oxygen over stoichiometry which both contribute to the incommensurability of these oxides. Note that this evolution is not perfectly continuous, due to the fact that the oxygen stoichiometry of these oxides is highly sensitive to the oxygen pressure and consequently to the thermal treatment especially temperature. It is also worth pointing out that for x> 0.375 a small fraction of dimeric units

"MM'O_6"may coexist with trimeric units as shown for x=0.40 for which 0.8% of dimeric units is detected.

Concluding remarks

This study shows the primordial role of oxygen over stoichiometry in the system $Sr_{1+x}(Mn_{1-x}Co_x)O_{3+\delta}$ opening a broad field for the generation of a large family of aperiodic structures $Sr_{1+y}[(Mn_{1-x}Co_x)_{1-z}\square_z]O_3$,whose chains of face-sharing octahedra and trigonal prisms are built up of two sorts of polyhedral units, M_3O_9 and M_4O_{12}. The detailed structure determination of the commensurate oxide $Sr_4(Mn^{IV}_{1.818}Co^{III}_{0.544}\ Co^{II}_{0.548}\square_{0.09})O_9$ clearly establishes the presence of cationic vacancies on the trigonal prismatic sites. This point is of capital importance, since it allows the effect of oxygen over-stoichiometry on the commensurability/incommensurability of the structure to be explained, depending on the synthesis conditions. Importantly, these results demonstrate that the nature and the proportion of polyhedral units, the rate of cationic vacancies(z) in the chains, as well as the Co^{2+}/Co^{3+} content (i.e. oxygen over-stoichiometry δ) can be directly deduced with a high accuracy from the simple measurement of the modulation vector on PXRD patterns.

Although the magnetic study is out of the scope of the present paper, let us emphasize the high impact of these results on the magnetism of the Ising chain oxides. Several compositions of this $Sr_{1+x}(Mn_{1-x}Co_x)O_{3+\delta}$ system were previously investigated by different authors for their magnetic properties. These compounds were formulated as $Sr_4Mn_2CoO_9$ [30, 31, 32, 43], $Sr_9Mn_5Co_2O_{21}$ [41], and $Sr_{1+x}(Mn_{1-x}Co_x)O_3$. Unfortunately in those oxides no attention was paid for incommensurability in connection with a possible oxygen over-stoichiometry. As a result, the interpretation of the magnetic properties of all those compounds might be questionable. Our statement is strongly supported by the fact that in a recent study of the oxides $Sr_3CaMn_2CoO_{9+\delta}$ [45] which belong to this family, we have clearly shown changes in the magnetic response of the incommensurate oxides ($\delta \neq 0$) with respect to the commensurate stoichiometric oxide ($\delta = 0$). This phenomenon was assumed to originate from incorporation of extra oxygen into the commensurate oxide, leading to the replacement of some trimeric M_3O_9 units by tetrameric M_4O_{12} units with a concomitant appearance of cationic vacancies in the trigonal prismatic sites. Thus, for the understanding of the physics of Ising Chain magnets, it will be important in the future to characterize carefully their oxygen over-stoichiometry since it may induce a fragmentation effect of the chains.

In summary, a very efficient tool is now available for designing new spin chain oxides and for controlling their detailed structure, commensurate or not, and their chemical composition from the view point of oxygen over stoichiometry and cationic vacancies. The potential of these materials for creating new Ising magnet derivatives with various intra chain and inter chain interactions is high. Based on the concept of cationic vacancies associated with oxygen over stoichiometry substitutions of strontium by other alkaline earth cations and of the couple "Mn-Co" by other transition elements, will allow numerous other fragmented chain structures with various magnetic properties to be synthesized.

EXPERIMENTAL SECTION

Synthesis

The samples listed in Table 1and 5 were all synthesized in air by standard solid state reaction from stoichiometric mixtures of $SrCO_3$ (99.8%), Co_3O_4 (99.7%) and MnO_2 (99.99%), all being from AlfaAesar. The oxygen stoichiometry of the commercial cobalt oxide was determined to be $CoO_{1.32}$ instead of Co_3O_4 from thermogravimetric analysis. The appropriate proportions of the starting materials were weighted and thoroughly mixed with mortar pestle, adding ethanol for homogeneous mixing. The intimate mixtures were first heated 12 hours in air at 1000°C for de-carbonation. The samples were then reground and pressed under uniaxial pressure of ~3 ton in the form of parallelepipeds before being heated in air at 1400°C for 12 hours and finally quenched to room temperature. Importantly, the oxygen stoichiometry of the final materials is highly sensitive to the thermal treatment and particularly to the temperature and cooling method. For the sake of comparison a particular attention was paid to use the same protocol for the synthesis in order to avoid any variation of the oxygen pressure between the different samples. Crystals I were extracted from the batch corresponding to x= 3/8 (Table1). Crystal II (Table 3) were grown from a similar method but heating the mixture up to 1500°C instead of 1400°C.

The samples $Sr_{4/3}Mn_{2/3}Co_{1/3}O_{3+\delta}$, listed in Table 3 were also prepared from the stoichiometric mixture of oxides and carbonate preheated in air at 1000°C for 48hrs for decarbonation similar to the method described above. A large amount of the obtained mixture was carefully homogenized and heated up to 1200°C for 84hrs and then at 1250°C for 48hrs. The synthesized sample was divided into four parts: the "Pristine" sample used for a first structural and magnetic characterization and the three other parts that were annealed in different conditions. The A-Air sample was obtained by heating a pristine part in air up to 1425°C for 48hrs , while the A-Ar 1375°C and A-Ar 1420°C samples were obtained by annealing the pristine parts respectively at

the indicated temperatures for 20hrs. The Pristine and A-air samples were finally quenched down to room temperature.

The sample $Sr_{4/3}Mn_{2/3}Co_{1/3}O_3$ (δ=0) labeled ST (Table 3) was synthesized from a stoichiometric mixture of SrO, MnO_2, $CoO_{1.32}$ and metallic cobalt heated in sealed tube at 1150°C for 24hrs, using a glove box in order to avoid any carbonation of SrO before heating.

Estimation of the oxygen over stoichiometry: thermo-gravimetric analysis

Due to the very small deviation from "O_3" stoichiometry (see δ values listed in tables1, 3, 4, 5) chemical analysis using iodometric titration did not allow significant determination of the extra oxygen content in the samples. Thermo-gravimetric analysis was performed which could give a semi quantitative estimation of the oxygen excess (see SI-3) supporting the existence of excess oxygen deduced from the structural study.

X-ray diffraction measurements

The powder X-ray diffraction (PXRD) patterns were recorded with a D8 ADVANCE Vario1 (Bruker) diffractometer under a continuous scanning mode in the 2Θ range 10° to 140° and a step size $\Delta(2\Theta)$=0.00526° with Cu Kα1 radiation.

The single crystal data collections were performed using a 4-circles single crystal diffractometer Synergy S from RIGAKU equipped with a Mo photonjet microfocus source and an Eiger 1M HPC X-ray detector from Dectris. Once the two sub-lattices were identified, a list of the expected main and satellite reflections was generated using Jana2006 following the extinction rules of the super space group R-3m (00γ)0s. The list has been used by the software CrysalisPro for the integration. Details of the full process are given in supplementary materials.

High resolution electron microscopy study

The transmission electron microscopy investigations were performed on a JEOL F200 microscope operating at 200 kV and equipped with a bottom-mounted Gatan RIO16 camera. Samples were prepared by smoothly crushing samples under ethanol in an agate mortar and depositing drops of the mixture onto a holey carbon membrane supported by a Cu grid.

References

[1] J. Darriet and M.A. Subramanian, *J. Mater. Chem*., 1995, 5, 543-552.

[2] J.M. Perez-Mato, M. Zakhour-Nakhl, F. Weill and J. Darriet, *J. Mater. Chem.,* 1999, 9, 2795-2807.

[3] K. Boulahya, M. Parras and J.M. Gonzalez-Calbet, *J. Solid State Chem.,* 1999, 145, 116-127.

[4] K.E. Stitzer, J. Darriet and H.-C. zur Loye, *Curr. Opin. Solid State Mater. Sci.,* 2001, 5, 535-544.

[5] H.-C. zur Loye, Q. Zhao, D.E. Bugaris and W.M. Chance, *Cryst. Eng. Commun.,* 2012, 14, 23-39.

[6] S. Aasland, H. Fjellvåg and B. Hauback, *Solid State Commun.,* 1997, 101, 187-192.

[7] H. Kageyama, K. Yoshimura, K. Kosuge, M. Azuma, M. Takano, H. Mitamura and T. Goto, *J. Phys. Soc. Jpn.*, 1997, 66, 3996-4000.

[8] A. Maignan, C. Michel, A.C. Masset, C. Martin and B. Raveau, *Eur. Phys. J. B*, 2000, 15, 657-663.

[9] V. Hardy, S. Lambert, M.R. Lees and D. McK. Paul, *Phys. Rev. B*, 2003, 68, 014424-7.

[10] E.V. Sampathkumaran, N. Fujiwara, S. Rayaprol, P.R. Madhu and Y. Uwatoko, *Phys. Rev. B*, 2004, 70, 014437-4.

[11] V. Hardy, M.R. Lees, O.A. Petrenko, D. McK. Paul, D. Flahaut, S. Hebert and A. Maignan, *Phys. Rev. B*, 2004, 70, 064424-064427.

[12] V. Hardy, D. Flahaut, M.R. Lees and O.A. Petrenko, *Phys. Rev. B*, 2004, 70, 214439-7.

[13] H. Wu, M.W. Haverkort, Z. Hu, D.I. Khomskii and L.H. Tjeng, *Phys. Rev. Lett.*, 2005, 95, 186401-4.

[14] S. Agrestini, C. Mazzoli, A. Bombardi and M.R. Lees, *Phys. Rev. B,* 2008, 77, 140403(R).

[15] S. Agrestini, L.C. Chapon, A. Daoud-Aladine, J. Schefer, A. Gukasov, C. Mazzoli, M.R. Lees and O.A. Petrenko, *Phys. Rev. Lett.*, 2008, 101, 097207-4.

[16] Y.B. Kudasov, A.S. Korshunov, V.N. Pavlov and D.A. Maslov, *Phys. Rev. B*, 2008, 78, 132407-4.

[17] C. Mazzoli, A. Bombardi, S. Agrestini and M.R. Lees, *Physica B*, 2009, 404, 3042-3044.

[18] R. Soto, G. Martínez, M.N. Baibiche, J.M. Florez and P. Vargas, *Phys. Rev. B*, 2009, 79, 184422-8.

[19] Y.B. Kudasov, A.S. Korshunov, V.N. Pavlov and D.A. Maslov, *Phys. Rev. B*, 2011, 83, 092404-4.

[20] S. Agrestini, C.L. Fleck, L.C. Chapon, C. Mazzoli, A. Bombardi, M.R. Lees and O.A. Petrenko, *Phys. Rev. Lett.,* 2011, 106, 197204-4.

[21] Y. Kamiya and C.D. Batista, *Phys. Rev. Lett.,* 2012, 109, 067204-5.

[22] A. Jain, P.Y. Portnichenko, H. Jang, G. Jackeli, G. Friemel, A. Ivanov, A. Piovano, S.M. Yusuf, B. Keimer and D.S. Inosov, *Phys. Rev. B*, 2013, 88, 224403-5.

[23] G. Allodi, P. Santini, S. Carretta, S. Agrestini, C. Mazzoli, A. Bombardi, M.R. Lees and R. De Renzi, *Phys. Rev. B*, 2014, 89, 104401-5.

[24] P. Lampen, N.S. Bingham, M.H. Phan, H. Srikanth, H.T. Yi and S.W. Cheong, *Phys. Rev. B,* 2014, 89, 144414-8.

[25] Y.J. Jo, S. Lee, E.S. Choi, H.T. Yi, W. Ratcliff II, Y.J. Choi, V. Kiryukhin, S. W. Cheong and L. Balicas, *Phys. Rev. B,* 2009, 79, 012407-4.

[26] V. Kiryukhin, Seongsu Lee, W. Ratcliff II, Q. Huang, H.T. Yi, Y.J. Choi and S.- W. Cheong, *Phys. Rev. Lett.,* 2009, 102, 187202-4.

[27] T. Lancaster, S.J. Blundel, P.J. Blaker, H.J. Lewtas, W. Hayes, F.L. Pratt, H.T. Yi and S.W. Cheong, *Phys. Rev. B,* 2009, 80, 020409-4(R).

[28] Z.W. Ouyang, N.M. Xia, Y.Y. Wu, S.S. Sheng, J. Chen, Z.C. Xia, L. Li and G.H. Rao, *Phys. Rev. B,* 2011, 84, 054435-5.

[29] J.W. Kim, Y. Kamiya, E.D. Mun, M. Jaime, N. Harrison, J.D. Thompson, V. Kiryukhin, H.T. Yi, Y.S. Oh, S.W. Cheong, C.D. Batista and V.S. Zapf, *Phys. Rev. B,* 2014, 89, 0604045(R).

[30] K. Boulahya, M. Parras, J. M. Gonzalez-Calbet and J. L. Martinez, *Chem. Mater.,* 2003, 15, 3537-3542.

[31] Md. Motin Seikh, V. Caignaert, O. Perez, B. Raveau and V. Hardy, *Phys. Rev. B,* 2017, 95, 174417-6.

[32] Md. Motin Seikh, V. Caignaert, O. Perez, B. Raveau and V. Hardy, *J. Mater. Chem. C*, 2018, 6, 3362-3372.

[33] V. Hardy, V. Caignaert, O. Perez, L. Herve, N. Sakly, B. Raveau, Md. M. Seikh and F. Damay, *Phys. Rev. B*, 2018, 98, 144414-9.

[34] R. Sessoli, D. Gatteschi, A. Caneschi and M.A. Novak, *Nature*, 1993, 365, 141-143.

[35] See, for a Review: D. Gatteschi, R. Sessoli and J. Villain, *Molecular Nanomagnets*, Oxford University Press, Oxford, 2006.

[36] A. Caneschi, D. Gatteschi, N. Lalioti, C. Sangregorio, R. Sessoli, G. Venturi, A. Vindigni, A. Rettori, M.G. Pini and M.A. Novak, *Angew. Chem. Int. Ed*., 2001, 40, 1760-1763.

[37] See, for a review: C. Coulon, H. Miyasaka and R. Clerac, *Single-chain magnets: theoretical approach and experimental systems*, in: R. Winpenny and D. M. P. Mingos (Eds.), *122 Structure and Bonding*, Springer, 2006, pp. 163-206; (a) C. Coulon, V. Pianet, M. Urdampilleta and R. Clerac, *Single-chain magnets and related systems*, in: S. Gao and D. M. P. Mingos (Eds.), *164 Structure and Bonding*, Springer, 2014, pp. 143-184.

[38] M. Suzuki and R. Kubo, *J. Phys. Soc. Jpn.*, 1968, 24, 51-60.

[39] R. Stanley, in: *Phase Transition and Critical Phenomena*, Clarendon Press Oxford, 1971, p. 280. Appendix E.

[40] M.N. Leuenberger and D. Loss, *Nature*, 2010, 410, 789-793.

[41] K. Boulahya, M. Parras, J. M. Gonzalez-Calbet and J. L. Martinez, *Chem. Mater.,* 2004, 16, 5408-5413.

[42] N. A. Jordan, P.D. Battle, S. van Smaalen and M. Wunschel, *Chem. Mater.,* 2003, 15, 4262-4267.

[43] M. A, Melkozerava and G. V. Bazuev, *Russian J. Inorg. Chem.,* 2006, 51, 362-367.

[44] T. K. Mandal, A. M. Abakumov, J. Haderman, G. Van Tendeloo, M. Croft and M. Greenblatt, *Chem. Mater.,* 2007, 19, 6158-6167.

[45] Md. Motin Seikh, V. Caignaert, N. Sakly, O. Perez, B. Raveau and V. Hardy, *J. Alloys Compd.*, 2019, 790, 572-576.

[46] K. E. Stitzer, W. H. Henley, J. B. Claridge, H.-C. zur Loye and R. C. Layland, *J. Solid State Chem.,* 2002, 164, 220-229.

[47] R. C. Layland and H.-C. zur Loye, *J. Alloys Compd*., 2000, 299, 118-125.

[48] B. Raveau, *Chem. Rec. Jap.,* 2017, 17, 569-583.

[49] K. Boulahya, M. Hernando, M. Parras and J. M. Gonzalez-Calbet, J. Mater. Chem., 2007, 17, 1620-1626.